Chapter

Evaluation of Steel Rebar in Concrete Using Electromagnetic Method

Dongfeng He

Abstract

The corrosion of steel reinforcing bar (rebar) is the leading cause of deterioration of concrete. In Japan, many railway bridges were built 40 years ago. It is necessary to develop easy-operation method to evaluate the corrosion of steel rebar. A project about the corrosion evaluation of steel rebar was started in 2015. In this project, we have two objectives: one is to evaluate the depth and the diameter of steel rebar in concrete; another is to evaluate the corrosion of steel rebar in concrete. We developed electromagnetic methods to do nondestructive evaluation of the steel reinforcing bar (rebar) in concrete. Using two probes and lower excitation frequencies of 3.8 and 4.2 kHz, the depth and the diameter of the steel reinforcing bar can be evaluated. Using higher excitation frequency of about 80 kHz, and the X, Y signals of the lock-in amplifier, where the X signal is the same phase signal with the AC excitation magnetic field and Y signal is the 90° phase different signal with the AC excitation magnetic field, we could evaluate the corrosion of steel rebar. A compact system with low power consumption of 0.5 W was developed, and we also did some field experiments using this system.

Keywords: steel reinforcing bar, electromagnetic method, concrete, corrosion, eddy current, nondestructive evaluation

1. Introduction

The corrosion of steel reinforcing bar (rebar) in concrete structures not only reduces the strength of the concrete structures but also causes the breakage of the concrete due to the volume increase of the corrosion products. The corrosion of steel rebar is the leading cause of deterioration of concrete. The periodic inspection of the steel rebar in concrete is necessary and important. Knowing the conditions of the steel rebar in concrete structures, such as the location, the depth, the diameter, and the corrosion status of steel rebar, is important for the safety evaluation of concrete structures.

In Japan, many railway bridges were built 40 years ago. It is necessary to develop easy-operation method to evaluate the corrosion of steel rebar. A project about the corrosion evaluation of steel rebar was started in 2015. In this project, we have two objectives: one is to evaluate the depth and the diameter of steel rebar in concrete; another is to evaluate the corrosion of steel rebar in concrete.

Ultrasonic method [1, 2], X-ray method [3, 4], magnetic flux leakage (DC field) method [5–7], electromagnetic induction (AC field) method [8–13], microwave radar system [14–16], and thermography technology [17–18] have been used to evaluate the break, the location, or the corrosion of the steel rebar in concrete.

Ultrasonic methods are often used to measure the crack of the concrete and the delamination between steel rebar and concrete. The advantage of ultrasonic method is its big detection depth till to several meters. The disadvantage of ultrasonic method is the noise caused by the reflection of stones in concrete.

Concrete scanning and imaging with X-ray can be used to get the position, diameter, and corrosion information of steel rebar in concrete. The advantage is its high spatial resolution. The disadvantage is its complex and high price and unsuitability for field experiments.

The magnetic flux leakage (MFL) method is mainly used to detect breaks in prestressing steel of pretensioned and post-tensioned concrete structures. The microwave radar systems can be used to detect the position and the covering depth of the steel rebar; however, the water or moisture in the concrete structures may influence the detection accuracy of the detection, and it is difficult to detect the second-layer steel rebar for the concrete with steel rebar grid. Thermography technology is not suitable to detect the steel rebar with deep depth.

Compared with other methods, the low-frequency electromagnetic induction method has the advantages of low cost and easy operation. It can be used to detect the covering depth and diameter of the steel rebar. For the low-frequency electromagnetic method, the moisture of concrete also has less influence to the detection results. However, the depth resolution or depth accuracy of commercial electromagnetic system is not good, which is difficult to be used to evaluate the diameter reduction of steel rebar due to corrosion.

We developed electromagnetic evaluation methods to detect the depth, the diameter, and the corrosion of steel rebar.

In this chapter, we will summarize our researches on the nondestructive evaluation of steel rebar. Firstly, we will give an introduction of the corrosion mechanism and the corrosion products of the steel rebar in concretes; secondly, we will describe the setup and results of depth and diameter measurements using dual-frequency and dual-probe method; thirdly, we will discuss the experiments and results of corrosion evaluation of steel rebar; and finally, we will provide the conclusion.

2. Corrosion mechanism, corrosion products, and electromagnetic method

The corrosion of steel rebar in concrete is complex, but basically it is an electrochemical reaction similar to that of a simple battery. **Figure 1** shows the corrosion mechanism of steel rebar in concrete with seawater environment. The corrosion of steel rebar has strong relation with the PH value of the environment in concretes. The corrosion of the steel reinforcement occurs below pH 11. Initially, on the surface of steel rebar, a protective oxide coating is formed giving a pH of 13–14 adjacent to the steel. When the carbonation and chloride ions diffuse through the concrete and reach the embedded steel rebar, then the pH is lowered by the presence of the chloride ions. This corrosion process also requires oxygen diffused through the concrete, setting up an electrochemical reaction. The process is increased by the existence of voids in the concrete adjacent to steel.

As the corrosion process progresses, corrosion products tend to build up in certain areas of the steel rebar. These corrosion products have different elemental compositions than the original state.

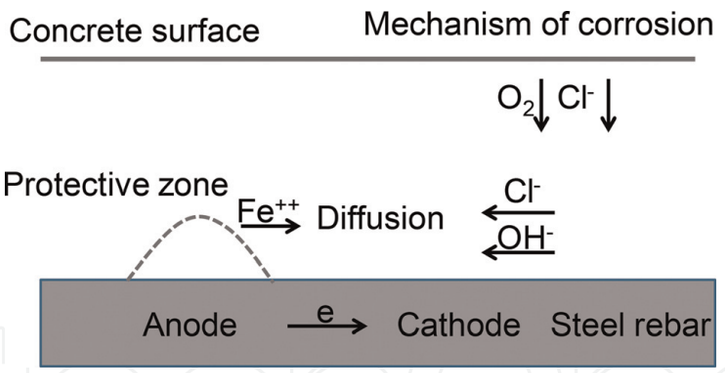

Figure 1.
Corrosion mechanism of steel rebar in concrete.

	Relative permeability	Conductivity (S/m)
Steel rebar	100	7×10^4
$FeO{\cdot}nH_2O$ ($Fe(OH)_2$)	1.0072	300
FeOOH (α, β, γ, δ)	1.1	5×10^{-9}
$Fe_2O_3{\cdot}H_2O$ ($Fe(OH)_3$)	Hundreds (soft)	10^{-4}
Fe_3O_4	Hundreds (hard)	200

Table 1.
Corrosion products and their electrical conductivities and permeabilities.

Almeida et al. [19] reported that the initial stages of atmospheric corrosion of carbon steel in both rural and urban atmospheres yield the formation of lepidocrocite (γ-FeOOH) and goethite (α-FeOOH). In chloride-containing environments, another form of iron oxyhydroxide, akaganeite (β-FeOOH), is frequently found [20]. Magnetite (Fe_3O_4) is also frequently reported in coastal environments [21]. Lepidocrocite and goethite are reported as the main phases independent of the environment [22]. Raman spectroscopy has been successfully used to characterize the different oxide phases formed on iron-based alloys [23]. What we normally call rust is a flaky red-brown solid which is largely hydrated iron. The primary corrosion product of iron is $Fe(OH)_2$ (or more likely $FeO{\cdot}nH_2O$), but the action of oxygen and water can yield other products having different colors: $Fe_2O_3{\cdot}H_2O$ (hydrous ferrous oxide, sometimes written as $Fe(OH)_3$) is the principal component of red-brown rust. It can form a mineral called hematite. $Fe_3O_4{\cdot}H_2O$ ("hydrated magnetite" or ferrous ferrite, $Fe_2O_3{\cdot}FeO$) is most often green but can be deep blue in the presence of organic complexants as shown here. Fe_3O_4 ("magnetite") is black.

These corrosion products are on the surface of the steel rebar and have different electrical conductivities and permeabilities. **Table 1** shows several kinds of corrosion products and their electrical conductivities and permeabilities.

Steel rebar has high permeability and high electrical conductivity. All the corrosion products have lower electrical conductivity than steel rebar. For some corrosion products, such as $FeO{\cdot}nH_2O$ and FeOOH, the permeabilities become smaller, and the relative permeabilities are close to 1; for some corrosion products, such as $Fe_2O_3{\cdot}H_2O$ and Fe_3O_4, the permeabilities become bigger. $Fe_2O_3{\cdot}H_2O$ is a kind of soft magnetic material, and Fe_3O_4 is a kind of hard magnetic material. Because of the different electrical conductivity and permeability properties, the electromagnetic responses of these corrosion products are different. Therefore, it is possible to evaluate the corrosion of steel rebar using electromagnetic method.

Figure 2 shows the principle of electromagnetic method to evaluate the steel rebar. AC magnetic field is produced by the excitation coil when AC current flows

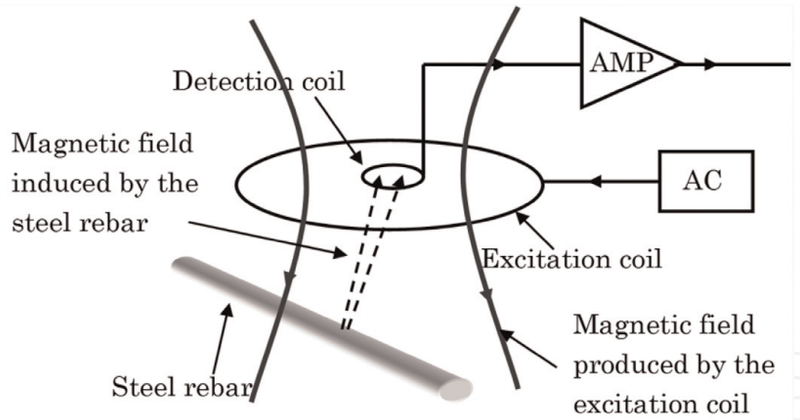

Figure 2.
Principle of electromagnetic method.

in it. Then, eddy current and magnetization are caused in the steel rebar. The detection coil is used to measure the magnetic field produced by the eddy current and the magnetization of steel rebar. The penetration depth of the eddy current has relation with the frequency, the electrical conductivity, and permeability of the material. It can be expressed by this formula:

$$\delta = \frac{1}{\sqrt{\pi f \mu \sigma}} \tag{1}$$

where δ is the penetration depth, f is the frequency, μ is the permeability, and σ is the electrical conductivity. When low-frequency electromagnetic field is used, the penetration depth of eddy current is big, and the magnetization effect which determines the signal, depth, and diameter of steel rebar can be evaluated. When high-frequency electromagnetic field is used, the penetration depth is small; mainly, the surface property of steel rebar determines the signals; thus the corrosion of steel rebar can be evaluated. For steel rebar, the relative permeability μ_r is about 100. The electrical conductivity is about 7×10^6 S/m. Using Formula (1), we can calculate the penetration depth. It is about 0.32 mm when the frequency is 4 kHz, and it is about 0.07 mm when the frequency is 80 kHz.

We find the magnetization effect has more contribution to the signal at 4 kHz, so we will use the frequency of about 4 kHz to evaluate the depth and diameter of steel rebar. And the eddy current effect has more contribution to the signal, and the penetration depth is small at 80 kHz, so we will use the frequency of about 80 kHz to evaluate the corrosion of steel rebar.

3. Depth and diameter detection of steel rebar

To measure the depth and the diameter of steel rebar simultaneously, two probes and dual-frequency method were used. **Figure 3** shows the setup of the measuring system.

For each probe, it was composed by a signal generator, an excitation coil, and a detection coil. The signal generators were used to produce the AC current and sent to the excitation coils to produce the AC magnetic fields. The magnetic fields induced by the steel rebar due to the eddy current and the magnetization were detected by the detection coils. The output signals of the detection coils were amplified by the amplifiers. The demodulators were used to get the amplitudes of

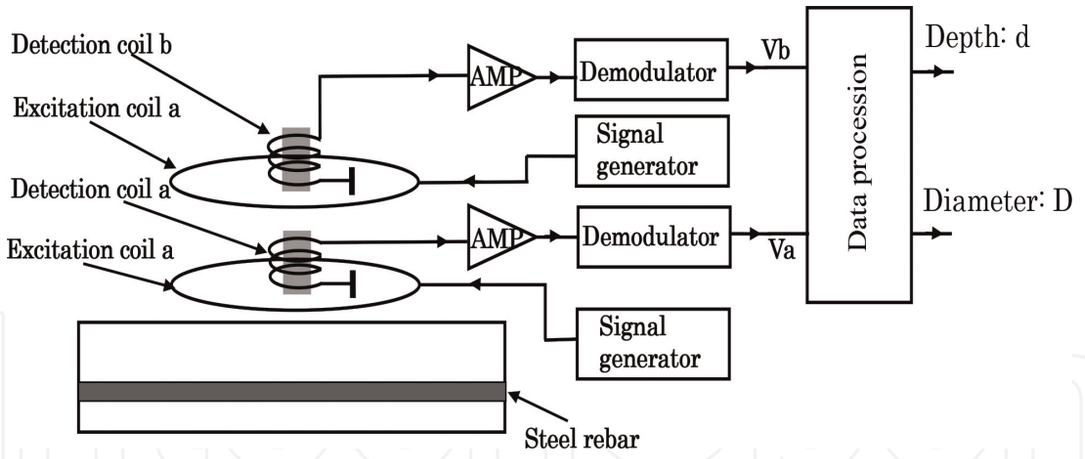

Figure 3.
Experimental setup for the depth and diameter evaluation of steel rebar.

Depth (mm)	Diameter (20 mm)	Diameter (16 mm)	Diameter (13 mm)	Diameter (10 mm)
20	1.03142	0.85424	0.61139	0.37896
30	0.28668	0.23217	0.1742	0.10764
40	0.1011	0.08372	0.06353	0.04016
50	0.04279	0.03493	0.02726	0.01713
60	0.02003	0.01641	0.01276	0.00846
70	0.0101	0.00839	0.00651	0.00419
80	0.00555	0.00449	0.0036	0.0023
90	0.00312	0.0026	0.00201	0.0014
100	0.00188	0.00155	0.00133	0.00095

Table 2.
Signal amplitudes of V_a of probe a for the steel rebars with different diameters and depths.

the signals. After the data processing and calculation, the covering depth and the diameter of steel rebar were calculated.

The experimental conditions were as follows: the diameters of the two excitation coils were both 70 mm with the turns of 100. The two detection coils were both 200 turns with the diameter of about 10 mm. The gains of the amplifiers were 20 dB. The distance between the two detection coils was about 10 mm. The current amplitudes of the AC currents flowing in the excitation coils were both about 20 mA. To reduce the interference between the two probes, different frequencies were used for the two probes. The frequency of signal generators were 3.8 and 4.2 kHz, respectively, and low-pass filters were used after the demodulators.

For the steel rebar with different depths and different diameters, the amplitudes V_a and V_b of the output signals of the two probes were different. **Table 2** shows the signal amplitudes of V_a for the steel rebars with different diameters of 10, 13, 16, and 20 mm and depths from 20 to 100 mm. **Table 3** shows the signal amplitudes of V_b for the steel rebars with different diameters and depths.

Figure 4a and **b** shows the signal amplitudes V_a and V_b changed with the depths for different steel rebar diameters of 10, 13, 16, and 20 mm.

Figure 5a and **b** shows the signal amplitudes of V_a and V_b changed with the diameter of steel rebar with the depth of 30 mm. We can see the signals increased almost linearly with the diameter of the steel rebar. For other depths, the results were similar.

Depth (mm)	Diameter (20 mm)	Diameter (16 mm)	Diameter (13 mm)	Diameter (10 mm)
20	0.68276	0.55748	0.40017	0.25621
30	0.23165	0.18534	0.13871	0.08838
40	0.09557	0.07794	0.05806	0.03805
50	0.04572	0.03646	0.02731	0.01843
60	0.02359	0.01877	0.01402	0.0093
70	0.01261	0.01025	0.00731	0.00531
80	0.00723	0.00589	0.00447	0.00314
90	0.00453	0.00352	0.00253	0.00192
100	0.00301	0.00219	0.00162	0.00123

Table 3.
Signal amplitudes of V_b of probe b for the steel rebars with different diameters and depths.

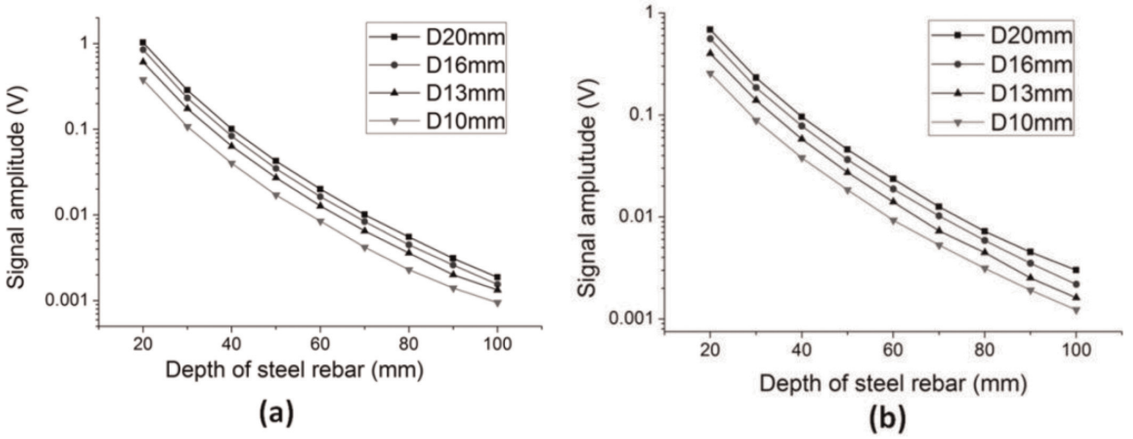

Figure 4.
(a) For different diameters of steel rebar, the signal amplitude of V_a changed with the depth of steel rebar. (b) For different diameters of steel rebar, the signal amplitude of V_b changed with the depth of steel rebar.

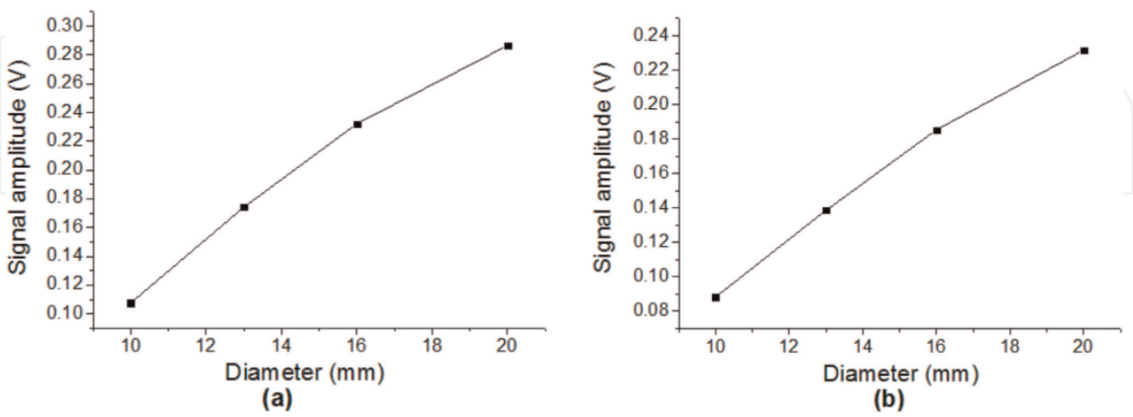

Figure 5.
(a) Signal amplitudes of V_a changed with the diameter of steel rebar with the depth of 30 mm. (b) Signal amplitudes of V_b changed with the diameter of steel rebar with the depth of 30 mm.

According to the data of **Tables 1** and **2**, a fitting formula was given to express the signal amplitudes changing with the diameter and the depth of steel rebar. The signal amplitude V_a of the lower probe was expressed by Formula (2):

$$V_a = kD \cdot e^{\left(-\beta d + \frac{\gamma}{\delta + d}\right)} \tag{2}$$

If the distance between the lower probe and the upper probe was L, the signal amplitude V_b of the upper probe was expressed by Formula (3):

$$V_b = kD \cdot e^{\left(-\beta(d+L) + \frac{\gamma}{\delta + d + L}\right)} \tag{3}$$

where V_a was the output signal amplitude of the lower probe and V_b was the output signal amplitude of the upper probe. D was the diameter of steel rebar, and d was the covering depth of steel rebar. L was the distance between the lower probe and the upper probe. α, β, and γ were constants.

Using Formulaa (2) and (3), we can get:

$$\frac{V_a}{V_b} = e^{\beta L} \cdot e^{\left(\frac{\gamma}{\delta + d} - \frac{\gamma}{\delta + d + L}\right)} = e^{\beta d_0} \cdot e^{\frac{\gamma L}{(\delta + d) \cdot (\delta + d + L)}} \tag{4}$$

From Formula (4), V_a/V_b was mainly determined by the covering depth of steel rebar, and it had less relation with the diameter of steel rebar.

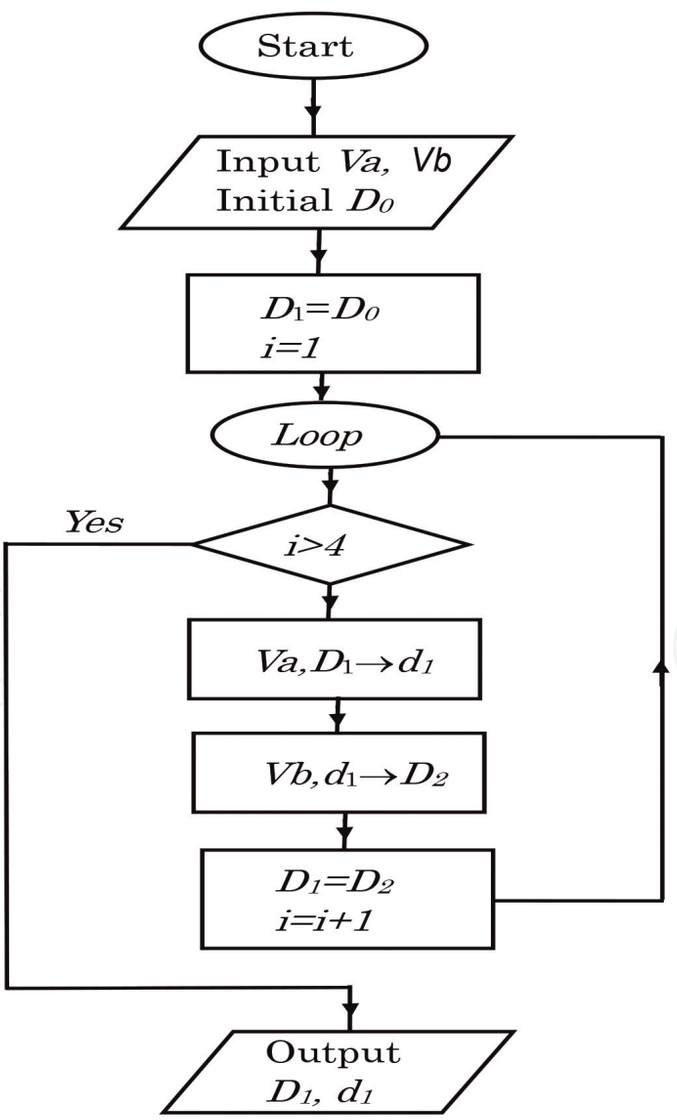

Figure 6.
Program flowchart of the recursion calculation method to get the depth and the diameter of the steel rebar.

For a steel rebar with unknown depth and diameter, V_a/V_b was obtained using the measured values of V_a and V_b. The covering depth d can be calculated using Formula (4), and the diameter D can be calculated using Formula (2) and the calculated depth d.

We can also calculate the depth d and the diameter D of the steel rebar using a recursion calculation method. **Figure 6** shows the program flowchart of the recursion calculation method. In the chart, D means the diameter of the steel rebar, and d means the depth of the steel rebar. First, set the diameter D_1 equal to the initial value of D_0. Then, use V_a and D_1 to calculate the depth of d_1, use V_a and d_1 to calculate D_2, and then repeat the calculation. The recursion calculation ended after calculating four times. Finally output the values of depth d_1 and the diameter D_1.

The result using the recursion calculation method and the calculation result using Formulas (1)–(3) were similar.

Table 4 shows the real values and the measured values of the depth and diameter of steel rebar using the recursion calculation method. For the steel rebar with depth of about 50 mm, the error of the depth measurement was about 0.5 mm, and the error of the diameter measurement was about 1 mm.

Real diameter (mm)	Real depth (mm)	Measured diameter (mm)	Measured depth (mm)
10	20	10.73	20.45
	30	10.30	30.35
	40	09.73	39.60
	50	09.65	49.50
	60	09.02	58.20
13	17	13.35	17.33
	27	12:48	28.83
	37	12.01	36.55
	47	12.16	46.58
	57	12.14	56.50
	67	11.50	65.45
16	14	15.11	14.24
	24	15.35	23.60
	34	15.12	33.65
	44	16.80	44.45
	54	15.05	53.60
	64	16.63	62.97
20	10	19.91	10.55
	20	20.67	19.85
	30	19.67	29.82
	40	20.09	39.80
	50	19.05	49.50
	60	19.24	60.75

Table 4.
Real values and measured values of the depth and diameter of steel rebar.

4. Corrosion evaluation of steel rebar

When corrosion happened with the steel rebar in concrete, corrosion products were produced on the surface of the steel rebar. The corrosion products had different electrical conductivity and permeability, so the electromagnetic response of the corrosion products was different from that of the steel rebar. Therefore, it was possible to evaluate the corrosion of steel rebar by measuring the electromagnetic response. **Figure 7** shows the experimental setup for the corrosion evaluation of steel rebar using electromagnetic method.

The excitation coil was used to produce the AC magnetic field, and eddy current was induced in the steel rebar. The detection coil was used to measure the magnetic field produced by the steel rebar. The lock-in amplifier was used to get the X and Y signal, where the X signal was the same phase signal with the excitation magnetic field and the Y signal was the 90° phase different signal with the excitation magnetic field.

Figure 8 shows the compact system of corrosion evaluation of steel rebar. The excitation coil, the detection coil, the amplifier, and the lock-in amplifier were integrated in a small box of about 9 × 12 × 7 cm. Only one USB cable was used to

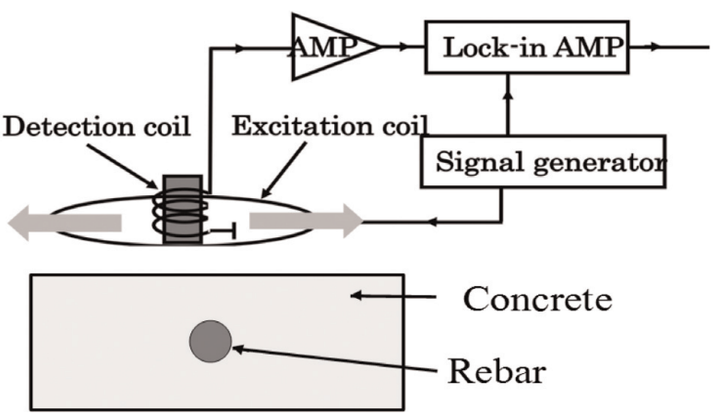

Figure 7.
Experimental setup for the corrosion evaluation of steel rebar using electromagnetic method.

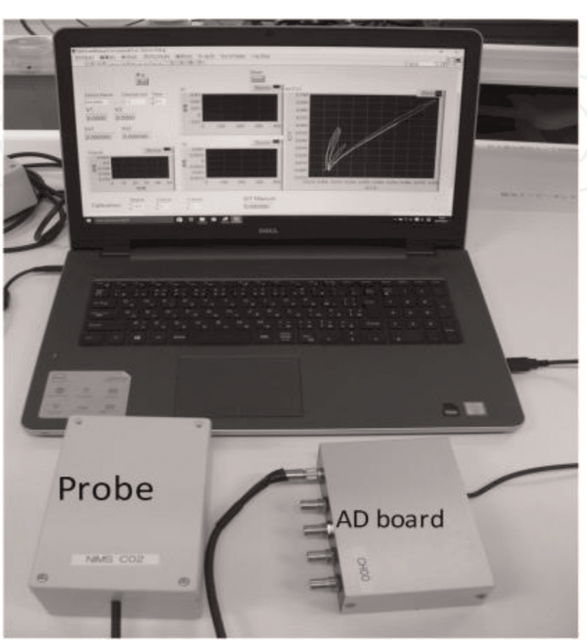

Figure 8.
Compact system for the corrosion evaluation of steel rebar.

connect it with a computer. The power of the system was also from the USB cable. The total power consumption of the system was about 0.5 W.

Figure 9 shows the samples of steel rebar with different corrosion levels. The diameter of the steel rebar was 16 mm. The steel rebar "*a*" had no corrosion; steel rebar "*b*" had a little corrosion, and there are some corroded dots on the surface the steel rebar; steel rebar "*c*" had big corrosion, and the thickness of the corroded layer was about 0.1 mm; and steel rebar "*d*" had severe corrosion with the thickness of the corrosion layer of about 1 mm.

In our experiments, the diameter of the excitation coil was 3 cm with 100 turns. The diameter of the detection was 1 cm with 100 turns. The frequency was 80 kHz and the current amplitude was 20 mA. We scanned the steel rebars using the system. **Figure 10** shows the signals of steel rebar with different depths of 2, 3, 4, and 5 cm.

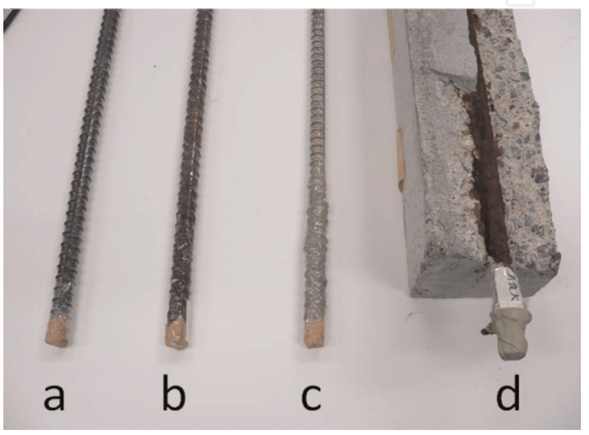

Figure 9.
Samples of steel rebar. (a) No corrosion, (b) a little corrosion, (c) big corrosion, and (d) severe corrosion.

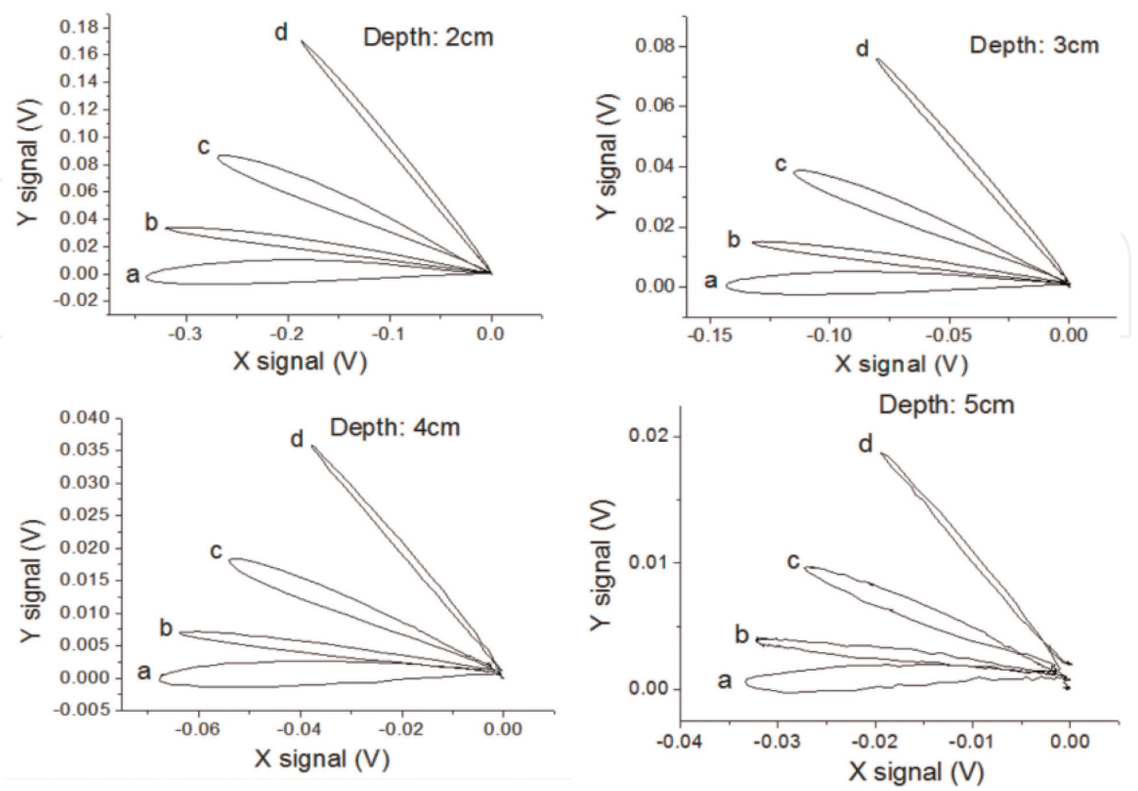

Figure 10.
Signals of steel rebars of (a), (b), (c), and (d) with different depths of 2, 3, 4, and 5 cm.

X-Y graphs were plotted using the X and Y output signals of the lock-in amplifier. The depth only changed the signal amplitudes of the X and Y signals, and it almost had no influence to the slope of the X-Y graph. For different corrosion levels, the slopes were different. From the slope, the corrosion of steel rebar can be judged.

The absolute value of ΔY/ΔX increased with the corrosion level. **Figure 11** shows the absolute values of ΔY/ΔX for the steel rebars at different depths. They were mainly determined by the corrosion levels and had less relation with the covering depth. This result proved that it was possible to evaluate the corrosion of steel rebar using this electromagnetic method.

We also did some field experiments using our system. The depths of steel rebars were measured. **Figure 12** shows it. The experiments were done under a railway bridge. When train passed over the bridge, there was almost no influence to our experiments. We did the scanning by hand. After measurements, the concrete was removed, and the real depths of steel rebars were measured. Then compare the real values with the measured values using electromagnetic method.

The steel bars were crossed into a mesh. The distance between the steel rebar was about 20 cm. **Figure 13** shows the real values and the measured values of steel rebar. The numbers in parentheses were measured values. For some rebars, the measured depths were consistent well with the real depths. For some rebars, there were big differences between the real values and the measured values. We found the difference was small, and the steel rebar had almost no corrosion; when the difference was big, the steel rebar had corrosion. When the steel rebar was corroded, the electrical conductivity and the permeability changed, which caused the difference between the real value and the measured value.

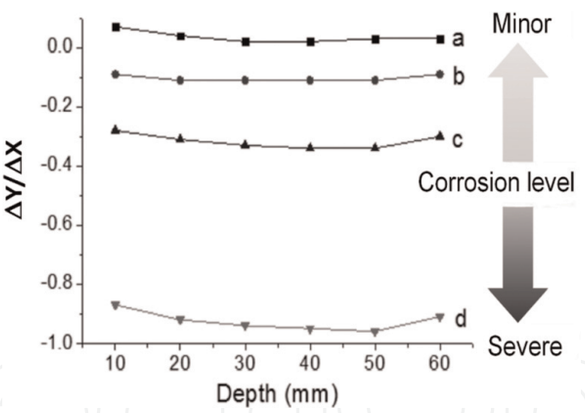

Figure 11.
Values of ΔY/ΔX for the steel rebars at different depths.

Figure 12.
Field experiments of checking the railway bridge.

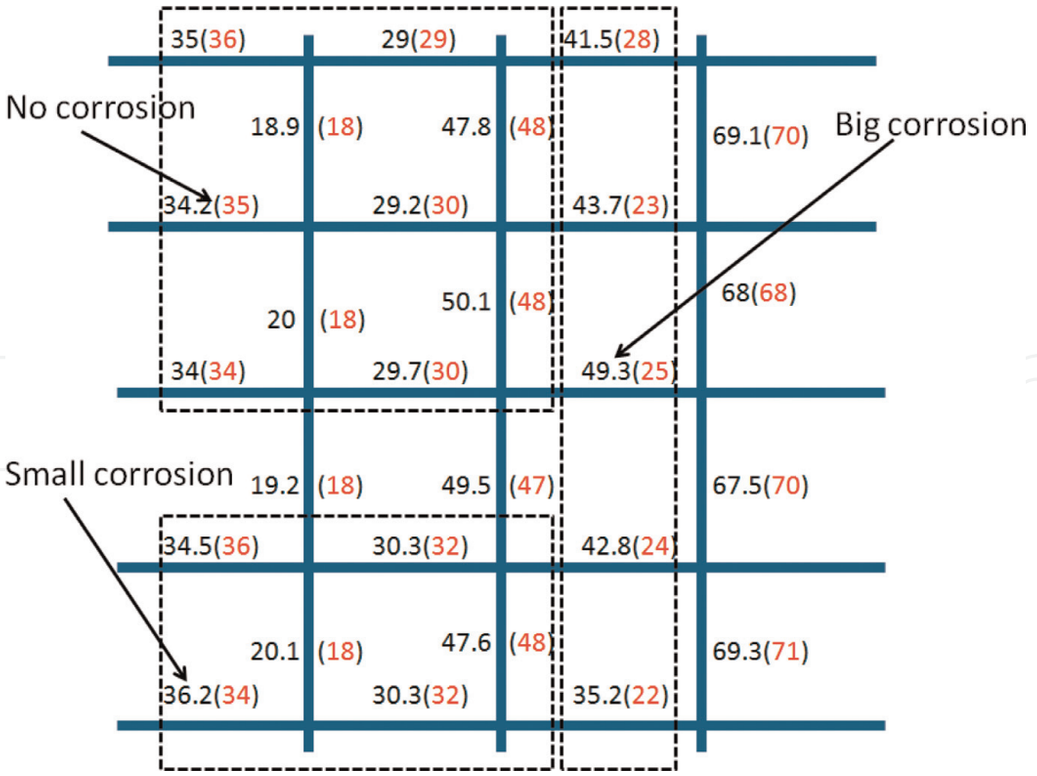

Figure 13.
Real values and the measured values of steel rebar. The numbers in parentheses were measured values. When the difference was big, the corrosion of steel rebar was also big.

5. Conclusion

Knowing the conditions of the steel reinforcing bar (steel rebar), such as the location, the diameter, and the corrosion of steel rebar, is important for the safety evaluation of concrete structures. We developed an electromagnetic method to detect the depth, the diameter, and the corrosion of steel rebar in concrete.

Using the lower frequencies of about 3.8 and 4.2 kHz and two probes, the depth and the diameter of steel rebar could be evaluated simultaneously. The resolution of about 1 mm was achieved.

Using higher frequency of about 80 kHz, the corrosion of steel rebar could be evaluated. A compact system with a low power of about 0.5 W was developed, and only one USB cable was used for the power and data transferring. The excitation coil, the detection coil, the amplifier, and the lock-in amplifier were integrated in a small box of about $9 \times 12 \times 7$ cm. Using the X signal and Y signal outputs of the lock-in amplifier, where the X signal is the same phase signal with the excitation current and the Y signal is 90° phase difference signal with the excitation current, we plotted X-Y graph of steel rebar signals. From the slope of the X-Y graph, the corrosion of steel rebar could be evaluated.

We also did some field experiments using our system. The depths of the steel rebar in a concrete railway bridge were evaluated. If the steel rebar had no corrosion, the measured value is consistent well with the real value. If the steel rebar had big corrosion, the difference between the real value and measured value was also big. The reason is that the corrosion products have different electromagnetic properties with the steel rebar. We will do more field experiments and improve our system in the future.

Acknowledgements

This work was supported by the Council for Science, Technology and Innovation, "Cross-ministerial Strategic Innovation Promotion Program (SIP), Infrastructure Maintenance, Renovation, and Management," (Funding agency: JST). We thank the helps from Dr. M. Shiwa, Dr. S. Takaya, Mr. S. Aramaki, Mr. N. Tsutsumi1, and Dr. K. Tsuchiya.

Author details

Dongfeng He
National Institute for Materials Science, Tsukuba, Japan

*Address all correspondence to: he.dongfeng@nims.go.jp

References

[1] Rucka M. Failure monitoring and condition assessment of steel-concrete adhesive connection using ultrasonic waves. Applied Sciences-Basel. 2018;**8**: article number 320

[2] Saleem M. Study to detect bond degradation in reinforced concrete beams using ultrasonic pulse velocity test method. Structural Engineering and Machanics. 2017;**64**:427-436

[3] Ostuka K, Takeda T. Research on internal shape detection of cracks in concrete structures. In: Proceedings of the 52nd JSCE Annual Meeting. Vol. V. 1997. pp. 692-693

[4] Beck M, Goebbels J, Burkert A, Isecke B, Babler R. Monitoring of corrosion processes in chloride contaminated mortar by electrochemical measurement and X-ray tomography. Materials and Corrosion. 2010;**61**:475-479

[5] Ghorbanpoor A. Magnetic-based NDE of steel in prestressed and post-tensioned concrete bridges. In: Proceedings Structural Materials Technology III. San Antonio, Texas; 1998. pp. 343-349

[6] Thomas W, Thomas V. Detection of reinforcement breaks on large-scale fatigue tests with the magnetic flux leakage method. In: 8th fib PhD Symposium in Kgs. Lyngby, Denmark; 2010. pp. 587-592

[7] Perin D, Goktepe M. Inspection of rebars in concrete blocks. International Journal of Applied Electromagnetics and Mechanics. 2012;**38**:65-78

[8] Gaydecki PA, Burdekin FM. An inductive scanning system for two dimensional imaging of reinforcing components in concrete structures. Measurement Science and Technology. 1994;**5**:1272-1280

[9] Yu ZZ, Gaydecki PA, Silva I, Fernandes BT, Burdekin FM. Magnetic field imaging of steel reinforcing bars in concrete using portable scanning systems. Review of Progress in Quantitative Nondestructive Evaluation. 1999;**18**:2145-2152

[10] Gaydecki P, Silva I, Fernandes BT, Yu ZZ. A portable inductive scanning system for imaging steel-reinforcing bars embedded within concrete. Sensors and Actuators A. 2000;**84**:25-32

[11] Miller G, Gaydecki P, Quek S, Fernandes B, Zaid M. A combined Q and heterodyne sensor incorporating real-time DSP for reinforcement imaging, corrosion detection and material characterization. Sensors and Actuators, A: Physical. 2005;**121**:339-346

[12] Ricken W, Mehlhorn G, Becker W. Determining of the concrete cover thickness and the bar diameter in reinforced concrete with a method of eddy current testing. In: Proceeding International Symposium Non-Destructive Testing in Civil Engineering. Berlin, Germany; 1995. pp. 197-204

[13] Miller G, Gaydecki P, Quek S, Fernandes BT, Zaid MAM. Detection and imaging of surface corrosion on steel reinforcing bars using a phase-sensitive inductive sensor intended for use with concrete. NDT & E International. 2003;**36**:19-26

[14] Bungey JH, Millard SG. Radar inspection of structures. In: Proceedings of the Institution of Civil Engineers—Structures and Buildings. Vol. 99. 1993. pp. 173-178

[15] Molyneaux TCK, Millard SG, Bungey JH, Zhou JQ. Radar assessment of structural concrete using neural networks. NDT & E International. 1995; **28**:281-288

[16] Shaw MR, Millard SG, Molyneaux TCK, Taylor MJ, Bungey JH. Location of steel reinforcement in concrete using ground penetrating radar and neural networks. NDT & E International. 2005; **38**:203-212

[17] Keo SA, Brachelet F, Breaban F, Defer D. Steel detection in reinforced concrete wall by microwave infrared thermography. NDT & E International. 2014;**62**:172-177

[18] He Y, Tian G, Pan M, Chen D. Eddy current pulsed phase thermography and feature extraction. Applied Physics Letters. 2013;**103**:084104

[19] Almeida E, Morcillo M, Rosales B, Marrocos M. Atmospheric corrosion of mild steel part I—Rural and urban atmospheres. Materials and Corrosion. 2000;**51**(12):859-864

[20] Ma Y, Li Y, Wang F. Corrosion of low carbon steel in atmospheric environments of different chloride content. Corrosion Science. 2009;**51**(5): 997-1006

[21] Syed S. Atmospheric corrosion of hot and cold rolled carbon steel under field exposure in Saudi Arabia. Corrosion Science. 2008;**50**(6): 1779-1784

[22] Syed S. Atmospheric corrosion of carbon steel at marine sites in Saudi Arabia. Materials and Corrosion. 2010; **61**(3):238-244

[23] Hazan E, Sadia Y, Gelbstein Y. Characterization of AISI 4340 corrosion products using Raman spectroscopy. Corrosion Science. 2013;**74**:414-418